

Uncertainty Analysis for a Seismic Warning System

Allen L. Jones

Box 352700 Department of Civil & Environmental Engineering
University of Washington
Seattle, WA, 98195
Tel: 206-616-4393
Fax: 206-685-3836
email: jonesal@u.washington.edu

Steven L. Kramer

Box 352700 Department of Civil & Environmental Engineering
University of Washington
Seattle, WA, 98195
Tel: 206-685-2642
Fax: 206-685-3836
email: kramer@u.washington.edu

Pedro Arduino

Box 352700 Department of Civil & Environmental Engineering
University of Washington
Seattle, WA, 98195
Tel: 206-543-6777
Fax: 206-685-3836
email: parduino@u.washington.edu

Marc Eberhard

Box 352700 Department of Civil & Environmental Engineering
University of Washington
Seattle, WA, 98195
Tel: 206-543-4815
Fax: 206-543-1543
email: eberhard@u.washington.edu

Manuscript Word Count: 7,873

ABSTRACT

Following the collapse of the Cypress structure, which killed 42 people in the 1989 Loma Prieta earthquake, the Washington State Department of Transportation (WSDOT) initiated a series of studies of the seismic vulnerability of the Alaskan Way Viaduct (AWV). The AWV, which carries nearly 100,000 vehicles per day, is one of only two north-south highways through downtown Seattle. The studies showed that this double-deck structure is vulnerable to extensive damage during and shortly after strong earthquake shaking. The structural vulnerabilities, associated with reinforced concrete details typical of 1950's construction, are exacerbated by the presence of highly liquefiable soils beneath the AWV, and by the seismic vulnerability of a seawall that is located immediately west of the AWV.

To make decisions about closing the viaduct during or after an earthquake, WSDOT will need to have reliable and timely information about the likelihood of potential damage. In this context, the objective of this work was to develop design requirements for an instrumentation system that would detect the onset of soil liquefaction and provide input to a collapse warning system. Given the uncertainties associated with predictions of ground-shaking intensity, site response, liquefaction and structural performance, it is difficult to predict levels of damage accurately. Therefore, an important part of this study was the identification and quantification of sources of uncertainty that needed to be considered in the development of a criterion for collapse potential. A framework based on the total probability theorem was developed to evaluate the probabilities of failure. For each source, a conditional probability distribution function was developed across the anticipated range in values. The results take the form of probabilities of liquefaction-induced collapse as a function of triggering criteria.

INTRODUCTION

The Alaskan Way Viaduct (AWV), which carries nearly 100,000 vehicles per day, is one of only two north-south highways through downtown Seattle (Figure 1). The continuing operation of this 2.2 mi (3.5 km) long, double-deck structure is vital to the economic health of the Puget Sound region. The AWV also affects the physical well-being of many drivers and passengers. During commute hours, several thousand people can be on the AWV.

Several studies have indicated that the AWV could incur severe damage and possible collapse if an earthquake produces strong ground shaking at the site (Eberhard et al. 1995, Knaebel et al. 1995, Kramer et al. 1995). Despite the risk to life safety, sufficient funds to repair or replace the AWV have not been available to date. Until such funds become available and repair/replacement work is completed, the AWV will remain vulnerable. To reduce this threat, an investigation was conducted to develop an instrumented monitoring system that would (1) provide warning of at least one mechanism of impending AWV collapse, and (2) minimize AWV closure time following significant earthquakes by providing post-earthquake inspectors with quantitative information on bridge response and damage.

The objective of this study was to investigate the feasibility of a system that would reliably block or divert drivers from the AWV in the event of an earthquake with the potential to cause collapse. This paper describes the development of a warning algorithm for liquefaction-induced failure of the AWV.

Variability in subsurface soil conditions and ground motions, combined with uncertainties in the modeling of an existing seawall displacements, pile movements, and structural collapse, led to the development of probabilistic triggering criteria.

SEISMIC VULNERABILITY OF THE ALASKAN WAY VIADUCT

The seismic vulnerability of the AWV is influenced by many factors, including its location, age and construction. From the standpoint of geologic and geotechnical conditions, the AWV site is dominated by thick deposits of loose, saturated, cohesionless soils. Most of the loose soils were placed as fill during reclamation of Seattle's tide flats and extension of the Seattle waterfront toward Elliot Bay in the late 1800's and early 1900's. Toward the southern end of the AWV, the loose fill soils are underlain by loose, natural tide flat soils, which are similar to the fill soils in composition and behavior. The loose soils, which vary in thickness from zero to over 150 ft (46 m), are underlain by very dense sandy gravel and gravelly sand (glacial till).

The natural shoreline of Elliot Bay actually lies east of all but the very northern portion of the AWV; in other words, the current location of the AWV was part of Elliot Bay a century ago. The filling operations that extended the waterfront to its current position were typical of those used around the world at that time. The fill soils either were mixed with water and pumped to the site, or were dumped through waters of Elliot Bay. To retain the fill in a manner that would allow large ships to berth, the City of Seattle designed and constructed a timber and concrete seawall that runs parallel to much of the current alignment of the AWV about 100 ft (30 m) to the west. The seawall, constructed in the early 1930's with four different types of walls, was designed according to the procedures that were accepted at that time. Those procedures, however, did not account for increased lateral earth pressures caused by liquefaction.

The AWV, which is constructed nearly entirely of reinforced concrete, was built from 1949 to 1956 in three main sections. The northern third of the AWV consists of two side-by-side, single-deck structures. Near Pike Place Market, the AWV transitions to a double-deck configuration, which is maintained over most of the AWV. The northern two thirds were designed by the City of Seattle Engineering Department (SED), and the southern third was designed by the Washington State Department of Transportation (WSDOT).

Notwithstanding variations to accommodate off-ramps, superelevations and curves, the double-deck portion of the AWV consists mainly of three-span units that are separated from adjacent units by one-and-a-half and two-inch expansion joints. The two decks are supported by beams that run in the transverse direction (perpendicular to traffic) and deep girders that run in the longitudinal direction (parallel to traffic). The girders and columns form two frames that provide the unit's longitudinal lateral force resistance. In the transverse direction, the beams and columns form four frames that provide the lateral force resistance of the three-span unit (Figure 1).

The construction details of the AWV are typical of reinforced concrete bridges built before the 1971 San Fernando earthquake. The most significant difference between the AWV and modern bridges is the AWV's shortage of transverse reinforcement. Other differences include inadequate splice details, poorly confined joints and short anchorage lengths for positive beam reinforcement.

The AWV is supported on pile foundations that extend through the waterfront fill and tide flat deposits to the underlying dense soil (except for the southernmost portion for which pile driving records indicate that dense soils were not reached). Each column of the AWV is supported by a group of piles connected by a buried footing.

The number and arrangement of piles in each group vary along the length of the AWV, and between interior and exterior columns, and the sizes of the footings vary to accommodate the various pile groups. Available pile driving records indicate that most of the piles were driven only a short distance into the dense soil; consequently, pile-bearing support is derived from the top few feet of the dense soil.

SEQUENCE OF LIQUEFACTION-INDUCED FAILURE

Liquefaction-induced failure of the AWV would likely result from a series of related events. This sequence would begin with earthquake ground motion of sufficient intensity to cause liquefaction of the loose, saturated sands beneath the AWV and behind the seawall located immediately west of the AWV. The onset of liquefaction would then soften and weaken the soils thereby increasing the lateral earth pressure on the seawall. The seawall, which was not designed for the lateral earth pressure that would be imposed on it by liquefied soil, would begin to move outward toward Elliott Bay. Movement of the seawall would cause significant lateral soil movement at the location of the AWV; because of the variability of the soil, this movement would not occur uniformly. These variable soil movements would cause differential movement between the pile groups that support the AWV. This differential movement could cause the structure to collapse.

Some degree of uncertainty is associated with each step in the sequence of events leading to the potential collapse of the AWV. An important part of this study was the identification and quantification of these uncertainties for input into a collapse analysis. This approach required the development of a probabilistic framework that would relate the potential for collapse to the level of ground motion measured at the AWV. The primary sources of uncertainty include:

- 1) *Subsurface soil conditions in the general vicinity of critical areas of the AWV.* The properties of the loose, saturated soils vary along the AWV alignment and between discrete boring locations.
- 2) *Ground motions that could cause liquefaction.* Seismic hazards in the vicinity of the AWV can come from intraplate, interplate, and subduction zone sources. Because few strong ground motion records are available in the Pacific Northwest, particularly when compared to better-instrumented and more seismically active regions such as California, the uncertainty in ground motion amplitude, frequency content, and duration is significant.
- 3) *Residual strength of liquefied soil.* Accurate estimation of residual strength has proven to be very difficult. Residual strength is generally estimated from empirical correlations with SPT resistance and predict a wide range of residual strengths for a given SPT resistance.
- 4) *Seawall displacements.* The seawall, which includes a pile-supported relieving platform, is a complicated structure and its interaction with liquefying soil is also complex. Therefore, the displacement of the soil due to seawall movement is uncertain.
- 5) *Lateral pile displacement caused by free-field soil displacement.* Lateral movement of the soil surrounding the AWV foundations will cause those foundations to move. Soil-pile interaction analyses can provide an approximate, but not exact, estimate of the lateral displacements of the AWV foundations.
- 6) *Differential movement of AWV columns.* Differential displacements between adjacent pile-supported columns will induce potentially damaging deformation demands in the structure. Estimation of these demands requires characterization of uncertainty in differential foundation movement.
- 7) *Collapse displacement.* At some level of differential column displacement, brittle failure of one or more elements of the AWV superstructure could lead to collapse. Uncertainties in the design, construction, material properties, and behavior of the structure lead to uncertainties in estimates of the differential displacements required to cause collapse.

FRAMEWORK FOR WARNING CRITERION

A system intended to provide a warning of a potential collapse of a structure must have some criterion by which it is to be activated. The criterion must be expressed in terms of some quantitative parameter(s), e.g., in terms of a measured ground-motion parameter. The system could be designed to provide a warning when a threshold value of the ground motion parameter is reached. However, selection of the ground motion threshold must balance conflicting requirements. Ideally, it must (a) be low enough that all motions capable of causing collapse activate the warning system, (b) be high enough that the warning system is not activated by motions not capable of causing collapse, and (c) be of a form that can be determined as early as possible, so as to maximize the time available to react to the warning.

The previously described uncertainties must be considered in the development of a criterion for collapse potential. Therefore, the warning criterion had to be expressed probabilistically, i.e. in terms of the probability of collapse given the warning criterion. The goal was to determine threshold ground motion levels that give sufficient warning time and acceptable reliability of collapse prediction. Using the sequence of events leading to collapse, the following equation, based on the total probability theorem, describes the basic framework:

$$P[C|Y] = \sum P[C|d_{rel}]P[d_{rel}|d_{pile}]P[d_{pile}|d_{soil}]P[d_{soil}|S_r]P[S_r|L]P[L|Y] \quad (1)$$

where

$P[A/B]$ = probability of Event A given Event B,

C = collapse state,

Y = vector of ground motion parameters,

d_{rel} = relative pile displacement,

d_{pile} = displacement of pile head,

d_{soil} = free-field ground surface displacement at location of AWV,

S_r = residual strength of liquefied soil, and

L = initiation of liquefaction.

For a collapse warning system, the use of an integral parameter (i.e., one that reflects the cumulative “strength” of shaking as it builds up with time) to describe the ground motion is desirable. An integral parameter allows time rates of ground motion intensity to be easily computed from acceleration time histories; therefore, a warning system can be triggered when the parameter builds up to some threshold value. This parameter represents an important element of the vector of ground motion parameters, $[Y]$ used in Equation 1. The vector allows specification of a triggering criterion in terms of exceedance of a specified threshold value Y^* at a specified time, t^* . Figure 2 shows a particular triggering criterion (i.e., a particular $t^* - Y^*$ pair), along with plots of Y for two ground motions. For a given time, t^* , some events will generate sufficient energy to trigger a prediction of liquefaction by exceeding the specified level of Y^* . Less intense events will not generate the necessary intensity, as they are below the trigger level of Y^* .

UNCERTAINTIES IN EVALUATION OF LIQUEFACTION-INDUCED FAILURE POTENTIAL

The conditional probabilities listed in Equation 1 each represent the uncertainty in a parameter given the value of some other parameter. Each can be represented by a conditional probability distribution, the nature of which will directly influence the reliability with which the eventual probability of collapse, $P[C|Y]$, can be determined. This section presents a discussion of the sources of uncertainty considered in Equation 1. The approach was to identify and estimate the uncertainty in each parameter used in the analysis.

Liquefaction, $P[L, Y]$

Uncertainty in subsurface soil conditions was quantified by analyzing the results of SPT tests performed for the design of the AWV and for the seismic vulnerability evaluation reported by Kramer et al. (1995). These investigations indicated that the waterfront fill and tide flat deposit had a mean $(N_1)_{60}$ value of approximately 10, a standard deviation of approximately 4, and a scale of fluctuation of about 5 ft (1.5 m). To account for the variability in soil conditions with depth, these values were used to generate one-dimensional Gaussian random fields of $(N_1)_{60}$ values in the liquefiable portions of the soil profile. The soil profiles used for this study represented those at the critical sections of the AWV as identified by Kimmerling and Kramer (1996). These profiles consisted of 10 ft (3.1 m) of unsaturated sand underlain by 14 ft (4.3 m) of saturated, liquefiable sand (below the ground water table) and 200 ft (61.0 m) of very dense glacial till (silty, gravelly sand). Deterministic values of $(N_1)_{60}$ in the unsaturated sand and till were taken as 10 and 100, respectively. Other soil properties (shear wave velocity, soil friction angle, dilation angle, etc.) were directly computed from published SPT blow count correlations.

As indicated previously, triggering of the warning system required a ground shaking intensity criterion expressed in terms of a threshold ground motion intensity and time. Following the work of Kayen and Mitchell (1997), Arias intensity was selected as the ground motion parameter to be used for setting the triggering threshold. Arias intensity, defined for a single ground motion component as

$$I_a = \frac{\pi}{2g} \int_0^{\infty} [a(t)]^2 dt \quad (2)$$

is related to the cumulative energy dissipated by a population of single-degree-of-freedom systems subjected to that motion. Selection of potential threshold Arias intensity values, therefore, required evaluation of the rate at which Arias intensity would be expected to increase with time for ground motions that would be expected at the AWV.

A set of 161 recorded ground motions was developed for evaluation of liquefaction probabilities. To ensure that the durations of the ground motions were reasonable, the distribution of magnitudes of the earthquakes that produced these motions matched the distribution of magnitudes from de-aggregation of a probabilistic seismic hazard analysis (PSHA) for a nearby site. To ensure that the distribution of amplitudes were reasonable, the motions were scaled so that their peak accelerations were consistent with the distributions of peak accelerations (based on the PSHA) that would be expected within a 20-year period. These motions were then used as input motions to the computer program, WAVE, to compute the response of the critical soil profile. WAVE is a one-dimensional, nonlinear, effective stress-based site response analysis program. Originally developed by Horne (1996), it has been extended with a new constitutive model, *UWsand*, which captures important elements of liquefiable sand behavior in a manner that can easily be calibrated. For each ground motion, WAVE produced time histories of acceleration and pore water pressure distribution with depth; the acceleration time histories were used to compute time histories of Arias intensity.

The trigger for the warning system is expected to be based on ground motions measured by accelerometers located just below the liquefiable soil, as the intensity of the ground motion at that depth will reflect the level of shaking that the liquefiable soil will be subjected to. Computed pore water pressures from the WAVE analyses were averaged in the lower half of the liquefiable layer, which is where liquefaction would be expected to occur first. Because the potential for large deformation is of primary importance, liquefaction was considered to have occurred at a threshold of $r_u = 0.98$.

These conditional probabilities were computed for a number of I_a - t pairs; the results of the analyses are shown in Figure 3a, which shows that the probability of liquefaction for a given trigger time increases as the Arias intensity level increases, and that the probability of liquefaction for a given Arias intensity level decreases as the trigger time increases.

Residual Strength of Liquefied Soil, $P[S_r/L]$

Uncertainty in the residual strength of the soil was characterized using empirical relations by Seed and Harder (1990) in which the apparent residual shear strength was back analyzed from liquefaction-induced flow slides. Seed and Harder characterized the site conditions for each case history in terms of a single equivalent clean sand blow count. For the case of the AWV where average $(N_1)_{60} = 10$, the Seed and Harder chart predicts residual strength values of 100 – 400 psf (4.8 kPa – 19.2 kPa). Because little is known of the distribution of residual strength, a uniform distribution across the range of residual shear strength recommended by Seed and Harder was assumed.

Uncertainty in Lateral Soil Displacement, $P[d_{soil}|S_r]$

As described earlier, deterministic soil-structure interaction analyses of the seawall by Kimmerling and Kramer (1996) established an approximate relationship between the residual strength of the soil and soil displacement at the location of the AWV. The analyses showed that little soil displacement would be expected if the residual strength exceeded 1000 psf (47.9 kPa). For lower residual strengths, higher soil displacements are expected. At residual strengths of about 200 psf (9.6 kPa) or less, the analyses of Kimmerling and Kramer (1996) suggested catastrophic failure of the seawall with very large deformations. Although no probabilistic simulations of seawall deformations were performed by Kimmerling and Kramer, the approximate nature of the analyses indicate that considerable uncertainty should be assumed for the resulting displacement values; this uncertainty is expected to be higher for cases of lower residual strength (and higher displacement). Based on this interpretation, the total soil displacements were assumed to be lognormally distributed with a median value given by the results of Kimmerling and Kramer and a coefficient of variation (on the natural logarithm of displacement) that ranged linearly from 100% at a residual strength of about 100 psf (4.8 kPa) to 65% at a residual strength of about 800 psf (38.4 kPa). Based on the preceding assumptions, the resulting probability density function for total soil displacement, conditional on residual strength, can be computed as shown in Figure 3b.

Uncertainty in Total Pile Displacement, $P[d_{pile}|d_{soil}]$

Uncertainty in total pile displacement was modeled by considering the effect of total soil displacements imposed on the pile foundations. This was accomplished by considering the effect of soil profile variability and ground motion

variability as input to a non-linear pile-soil interaction analysis. The analysis was accomplished using the program DYNOPILE (Horne 1996; Arduino and Kramer, 2001). DYNOPILE is a one-dimensional soil-pile interaction model developed for the dynamic analysis of pile foundations. In DYNOPILE, the pile is modeled using a Beam-on-Nonlinear Winkler Foundation (BNWF) model. Nonlinear, inelastic, p - y curves are used to characterize the stiffness of the near-field model, while the model proposed by Nogami and Konagai (1992) is adopted for the far-field. Excitation was provided by the free-field displacement and velocities generated by WAVE. The p - y curves were degraded in accordance with the square root of effective confining pressure. The procedure used to determine the probability density function for pile displacements was as follows:

- 1) Ten random soil profiles were generated using procedures similar to those outlined for the subsurface soil conditions. The profiles were assumed to have initial static shear stresses corresponding to a slope of 3%.
- 2) Five ground motions were created by scaling a representative strong ground motion to peak accelerations of 0.1, 0.2, 0.3, 0.4 and 0.5 g.
- 3) Each profile was subjected to a one-dimensional site response analysis using WAVE to obtain the vertical distribution of final pore water pressure and the final free field soil displacement profile for the 50 combinations of subsurface conditions and ground motions. The soil free-field displacement at the ground surface was designated d_{soil} .
- 4) For each of the 10 random profiles generated in step 1), 10 nonlinear p - y curves were generated at each depth increment. The p - y curves were generated as functions of $(N_1)_{60}$ using procedures outlined in O'Neill and Murchison (1983). For each depth in each profile, p - y curves were generated assuming that $(N_1)_{60}$ values were normally distributed with $C.O.V. = 40\%$ about the value obtained from the random field simulation. For each profile, the final displaced shape of the pile was computed using DYNOPILE. For this analysis, an average pile diameter of 14 in (36 cm) was used to represent the typical AWW pile diameters of 12, 14, and 16 in (31, 36, and 41 cm). The final pile displacement at the ground surface was designated d_{pile} . The ratio of the displacement of the pile to ground surface soil displacement was computed for each of the 500 simulations.

Because the AWW piles are relatively flexible in bending, and because they extend through a significant thickness of non-liquefiable soil above the - 10 ft (3m)-deep water table, their displacement was not significantly different than the free-field soil displacement. The resulting probability density functions for pile displacement given soil displacement are shown in (Figure 4a).

Uncertainty in Relative Foundation Displacement, $P[d_{rel} / d_{pile}]$

Most multiple-supported structures, such as the AWW, are sensitive to relative displacements of their foundations. The results of the DYNOPILE analyses were also used to estimate uncertainty in the relative transverse displacement between pile caps, i.e. the differential pile displacements. The final pile displacements at the ground surface for each DYNOPILE simulation were compared to each other to characterize relative displacements, which are expressed in the form of a ratio between the differential displacements to the average total pile displacement for each pair of pile analyses. For example, the relative displacements for analyses i and j would be expressed as

$$d_{rel} / d_{pile} = 2 \left[\frac{d_j - d_i}{d_j + d_i} \right] \quad (3)$$

where d_i and d_j are the computed pile head displacements from analyses i and j , respectively. The initial factor of 2 was included, purely on the basis of judgment, to reflect the fact that the pile-soil interaction analyses did not capture all sources of differential foundation movement.

A histogram was generated from the relative displacements computed for all combinations of i and j . This information was used to construct the conditional probability distribution function shown in Figure 4b. Relative pile displacements were expected to occur in the range of 0 to 50 in (127 cm).

Uncertainty in Structural Failure, $P[C / d_{rel}]$

The vulnerability of the AWW structure to differential foundation displacements is difficult to estimate because numerous sources of uncertainty affect such estimates. The strengths of the structural materials, and the extent to which they vary along the length of the viaduct, are not known accurately. The AWW has a wide variety of geometric configurations and structural details, and to limit the scope of this study, many of these configurations and details were not considered. The 50-year age of the structure, as well as variations between the structural design and

the constructed structure, further cloud estimates of the actual state of the AWW. The timing of the pile-cap displacements also complicates the evaluation. These displacements would occur after a strong earthquake, so the relevant "initial" state at the beginning of the pile-cap displacement analysis is the state of the structure at the *end* of the strong shaking.

The vulnerability analysis is hindered also by the paucity of quantitative information on the accuracy of assessment methods for poorly detailed reinforced concrete structures. The few methods available have not been calibrated against a large number of tests, the methods were not developed for previously damaged structures, and the methods were not developed to predict structural collapse. In general, these methods were developed to predict less catastrophic levels of structural damage.

To keep the scope of the analysis manageable, structural calculations were performed only for the interior and exterior transverse frames of the SED typical unit (Figure 1). This unit, rather than the WSDOT unit, was selected for analysis, because previous analyses (Knaebel et al. 1995) had found that its columns were susceptible to shear failure, and because it is the type of unit encountered in the areas determined to be most susceptible to large, liquefaction-induced foundation movements. Only two failure modes were considered: shear failure of the first-story columns; and shear failure of the first-level beams (De la Colina et al. 1996).

The assessment strategy used in this work combines deterministic choices (e.g., selection of critical frames and failure modes), estimates of uncertainties (e.g., material strengths), and estimates of model inaccuracy (e.g., displacement ductility at onset of shear-strength degradation):

- For a particular pile-cap displacement, the vulnerability assessment was repeated 1000 times, each time with different sets of material properties, characteristics for the member demand analyses, and properties of the member fragility models. Table 1 lists the parameters that were varied, their mean values and their coefficients of variation (COV).
- **COLUMN DISPLACEMENT DUCTILITY DEMAND.** For a given pile-cap displacement and a particular set of analysis parameters, the displacement-ductility demands (μ) for the interior and exterior columns were estimated based on their effective column strengths and column stiffnesses. Column flexural strengths were determined from the results of Knaebel et al. (1995), whereas effective column stiffnesses were determined from nonlinear, plane-frame analyses using Dr. Frame (www.drsoftware.com). The coefficients of variation for column stiffness and strength were determined based on comparisons of measured and calculated force-displacement responses of columns tested in the laboratory (Eberhard and Parish 2001)
- **COLUMN-SHEAR FAILURE.** For each displacement-ductility demand, the prediction of column-shear failure was based on the degrading-shear-strength procedures proposed by Priestley et al. (1992), which are illustrated schematically in Figure 5a. Assumed coefficients of variation for the fragility parameters, reported in Table 1, were based solely on judgment.
- **BEAM-COLUMN CRACK OPENING.** Shear failure of the first-level beams was evaluated on the assumption that the beams would fail if a crack opened up sufficiently at the bottom of the beam at the beam-column interface. The relationship between pile-cap displacement and crack width was determined based on frame analysis (assuming stick members located at member centerlines) for three scenarios: (1) rigid beam-column joint (40% likelihood), (2) flexible beam-column joint (50% likelihood), and (3) flexible beam with hinges forming in beam end and at second-story splice (10% likelihood).
- **BEAM-SHEAR FAILURE.** For each beam-column crack width, shear failure was expected when the beam-column crack width exceeded, on average, 0.75 in (1.9 cm).
- **COMBINATION.** Failure by either mode in either frame was assumed to cause failure of the SED unit. Note that these analyses did not account for the large number of nominally identical frames in the viaduct. In effect, the analysis assumes that only one exterior and one interior frame would be subjected to large pile-cap displacements.
- The resulting fragility curves are shown in Figure 5b. According to these curves, the fragility of the unit is dominated by the column flexure-shear failure mode. The possibility of column-shear failure becomes significant at a displacement of approximately 10 in (25 cm). At a displacement of approximately 14 in (35 cm), the curves indicate that the likelihood of collapse is 50%.

RESULTS OF PROBABILISTIC ANALYSIS, $P[C / Y]$

The conditional probability density functions were used with Equation 1 to evaluate the probabilities of collapse for various triggering events as a function of I^* and t^* . The results are presented graphically in Figure 6, which shows the probability of collapse for various combinations of I^* and t^* . As an example, consider a threshold Arias intensity of $I^* = 0.33$ ft/sec (0.10 m/sec). If that level of shaking is reached in the first second of shaking ($t^* = 1.0$ sec), there is a 33% probability of liquefaction-induced collapse. If that level of shaking was not reached until $t^* = 5$ sec, however, the probability of liquefaction-induced collapse would drop to 24%. The probability of collapse will decrease as the time required to reach a given value of I^* increases.

Note that even when the probability of liquefaction is 100%, the probability of liquefaction-induced collapse would only be 35%. This condition represents an upper limit to the probability of liquefaction-induced collapse; it occurs because there are non-zero probabilities of small seawall movement, small relative soil displacement, and small pile movement that can combine to produce conditions in which the occurrence of liquefaction would not result in collapse.

Various combinations of I^* and t^* can produce the same probability of collapse. For a probability of collapse of 25%, for example, the triggering criteria could be set at $\{t^* = 1 \text{ sec}, I^* = 0.11 \text{ ft/s (0.03 m/s)}\}$ or $\{t^* = 5 \text{ sec}, I^* = 0.35 \text{ ft/s (0.11 m/sec)}\}$ or many other combinations of I^* and t^* . Although both triggering criteria lead to the same probability of collapse, the use of the former would allow a warning to be issued 5 sec earlier than the use of the latter. Such a time difference could be critical in reducing risks to the traveling public. This indicates that more accurate predictions of potential collapse can be made as the trigger time, t^* increases. While this may reduce the potential for a false trigger, it also reduces the time available for drivers to react to a collapse warning.

The specified acceptable level of risk and corresponding trigger values could be based on a benefit-cost analysis of the action levels for closing the AWV. This analysis would consider the costs associated with the effects of “false alarms” and missed events. The recommended triggering parameters would correspond to minimum total cost. In practice, foundation and structure displacements, as well as pore-water pressures, should be monitored directly to identify unexpected failures not predicted by a proposed algorithm. Such measurements could not replace a triggering algorithm, because they would provide little warning of failure, and the needed instrumentation could not be installed at all locations of potential failure.

CONCLUSIONS

Liquefaction-induced soil failures frequently take time to develop and can occur after earthquake shaking has ended. If the onset of liquefaction can be predicted at a relatively early point during a ground motion, the time between predictions and collapse can be used to take emergency measures. The purpose of the research described in this paper was to investigate the feasibility of a collapse warning system for the AWV in Seattle, and to identify criteria by which such a system could be triggered.

Because liquefaction-induced collapse of the AWV would involve a sequence of events, each of which is complex and has significant uncertainty associated with it, the potential triggering criteria were evaluated probabilistically. The process of identifying and characterizing the various sources of uncertainty, and combining them to obtain an estimated probability of collapse, led to the following conclusions:

- 1) While empirical procedures for practical evaluation of liquefaction potential are available and have been verified by field experience, procedures for characterization of the timing of liquefaction, which is critical for a warning system, have not been established.
- 2) A structure like the AWV could experience ground motions from earthquakes of various magnitudes and distances originating from various sources. Even for a given source, magnitude, and distance, record-to-record variability is high. Consequently, the uncertainty in ground motion characteristics, which influences the conditional probability of liquefaction, is very high.
- 3) Development of large soil deformations depend strongly on the residual strength of liquefied soil, which the geotechnical engineering profession is currently unable to estimate with much accuracy. As a result, the uncertainty in free-field displacement of liquefied soil is quite high.
- 4) The relatively flexible piles that support the AWV provide little resistance to soil deformation; consequently, they can be expected to move laterally with the liquefied soil. Hence, the uncertainty in pile displacement (given soil displacement) is quite low for this case.
- 5) Relative foundation displacements depend on the variability of subsurface conditions (e.g. soil thickness, density, etc.). Although the loose, saturated soils beneath the AWV are locally variable,

their thickness at a given bent are relatively constant. Site response analyses indicate that the relative displacements are relatively a small and moderately uncertain fraction of average pile displacement.

- 6) The potential for collapse of a complex structure due to relative movement depends on numerous factors. Even if the analysis is limited to a particular set of frames, as was the case for the Alaskan Way Viaduct, there are considerable uncertainties associated with a structure's initial state, including the extent of previous damage. There is also significant model inaccuracy, particularly for structures with potentially brittle details. For some parameters (e.g., the selection of critical failure modes), the analysis was treated deterministically. For others, the uncertainties and inaccuracies were considered explicitly based on the results of previous research (e.g., Eberhard and Parrish 2001) or on engineering judgment.
- 7) Combining all sources of uncertainty allows estimation of the probability of collapse for a given trigger criterion. This probability, and its variation with different trigger criteria, can be used to select specific trigger levels.

This research showed that a collapse warning system is feasible, but that significant uncertainty exists in the estimated probability of collapse for most reasonable trigger criteria. Selection of an optimum trigger criterion will require consideration of the costs and benefits associated with true and false collapse warnings.

ACKNOWLEDGEMENTS

Funding for this research was provided by the Washington State Department of Transportation. The support of this agency is gratefully acknowledged. The authors acknowledge the support provided by Chuck Ruth, Tim Moore, Ed Henley and Tony Allen.

REFERENCES

- Arduino, P., Kramer, S., Li, P. and D. Baska. *Dynamic Stiffness of Piles in Liquefiable Soils*. WA-RD 514.1, Washington State Department of Transportation, 2001.
- De la Colina, J., Eberhard, M.O., Ryter, S. and S. L. Wood. Sensitivity of Seismic Assessment of a Double-deck, Reinforced Concrete Bridge. *Earthquake Spectra*, Earthquake Engineering Research Institute, May 1996, Vol. 12, No. 2, pp. 217-244.
- Eberhard, M. O., De la Colina, J. and S. Ryter. *Seismic Vulnerability of the Alaskan Way Viaduct: WSDOT Typical Unit*. WA-RD 363.1. Washington State Department of Transportation, 1995.
- Eberhard, M.O. and M. Parrish. Accuracy of Performance Estimates for Reinforced Concrete Columns. *Proceedings, US-Japan Workshop on Performance-Based Design of Reinforced Concrete Structures*, Seattle, 2001.
- Horne, J.C. Effects of Liquefaction-induced Lateral Spreading on Pile Foundations. Ph.D. Dissertation, University of Washington, 1996.
- Kayen, R.E. and J. Mitchell. Assessment of Liquefaction Potential During Earthquakes by Arias Intensity. *Journal of Geotechnical and Geoenvironmental Engineering*, ASCE, 1997 Vol.123, No.12, pp. 1162-1174.
- Kimmerling, R.E. and S. Kramer. *Alaskan Way Viaduct: Phase III Seismic Vulnerability Study, Geotechnical Report*, Washington State Department of Transportation, 1996.
- Knaebel, P., Eberhard, M. O. and J. De la Colina. *Seismic Vulnerability of the Alaskan Way Viaduct: SED Typical Unit*. WA-RD 363.3. Washington State Department of Transportation, 1995.
- Kramer, S. L., Sivaneswaran, N. and K. Tucker. *Seismic Vulnerability of the Alaskan Way Viaduct: Geotechnical Engineering Aspects*. WA-RD 363.2. Washington State Department of Transportation, 1995.
- Nogami, T., Otani, J., Konagai, K. and H. L. Chen. Nonlinear Soil-pile Interaction Model for Dynamic Lateral Motion. *Journal of Geotechnical Engineering*, ASCE, 1992, Vol. 118, No.1, pp 89-116.
- O'Neill, M. and J. M. Murchison. *An Evaluation of p-y Relationships in Sands*. Research Report No. GT-DF02-83, University of Houston-University Park, 1983.
- Priestley, M. J. N., Seible, F. and Y. H. Chai. *Design Guidelines for Assessment Retrofit and Repair of Bridges for Seismic Performance*. Report No. SSRP-92/01. Department of Applied Mechanics and Engineering Sciences. University of California, San Diego, 1992.
- Seed, R.B. and L. F. Harder. SPT-based Analysis of Cyclic Pore Pressure Generation and Undrained Residual Strength. *Proceedings, H. Bolton Seed Memorial Symposium*, University of California, Berkeley, 1990, Vol. 2, pp. 351-376.

LIST OF TABLES AND FIGURES

TABLE 1 Parameter Variation for Calculation of Structural Fragility Curves

FIGURE 1 AWW Viaduct - Seattle, Washington.

FIGURE 2 Variation of Arias intensity with time relative to a particular trigger criterion.

FIGURE 3 Probability density functions: (a) liquefaction given Arias intensity, and (b) seawall displacement given residual strength.

FIGURE 4 Evaluation of uncertainty in relative foundation movement: (a) pile displacement given soil displacement, and (b) relative displacement given pile displacement.

FIGURE 5 Evaluation of uncertainty in structural behavior: (a) variation of column shear resistance with displacement ductility, and (b) structural fragility curves for typical SED unit.

FIGURE 6 Probability of collapse considering sources of uncertainty.

TABLE 1 Parameter Variation for Calculation of Structural Fragility Curves.

	Parameter	Assumed Mean Value	Assumed Variability
Material Properties	Concrete Nominal Compressive Strength, f_c	6300 psi	COV = 15%
	Steel Yield Stress, f_{sy}	36.3 ksi	COV = 10%
Column-Shear Demand Analysis	Column Effective Stiffness	88 k/in. (INT) 36 k/in. (EXT)	COV = 20%
	Column Flexural Strength	3200 k-ft (INT) 3000 k-ft (EXT)	COV = 10%
Priestley et al. (1992) Column-Shear Fragility Model	V_{ci}	$3.5 \sqrt{f'_c} 0.8 A_g$	COV = 10%
	V_{cf}	$1.2 \sqrt{f'_c} 0.8 A_g$	COV = 15%
	μ_i	2	COV = 10%
	μ_f	4	COV = 15%
	$V_s * (s * \tan 30) / (A_v * f_{sy} * D')$	1 for $\mu \leq \mu_i$ varies for $\mu_i < \mu \leq \mu_f$ 0 for $\mu > \mu_f$	COV = 0%
	V_p	$P \tan \alpha$	COV = 15%
Crack Opening Analysis	Crack Opening / Pile-Cap Displacement	0.01 0.03 0.06	40% 50% 10%
Beam-Shear Fragility Model	Critical Crack Opening	0.75 in.	COV = 25%

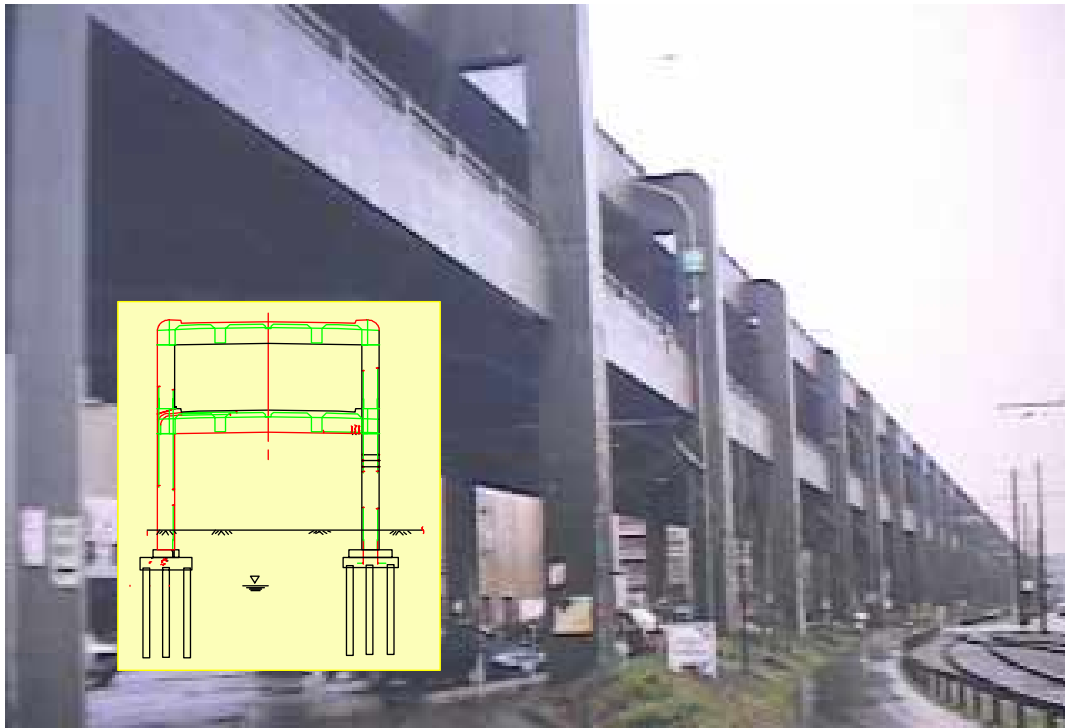


FIGURE 1 AWV Viaduct - Seattle, Washington (WSDOT).

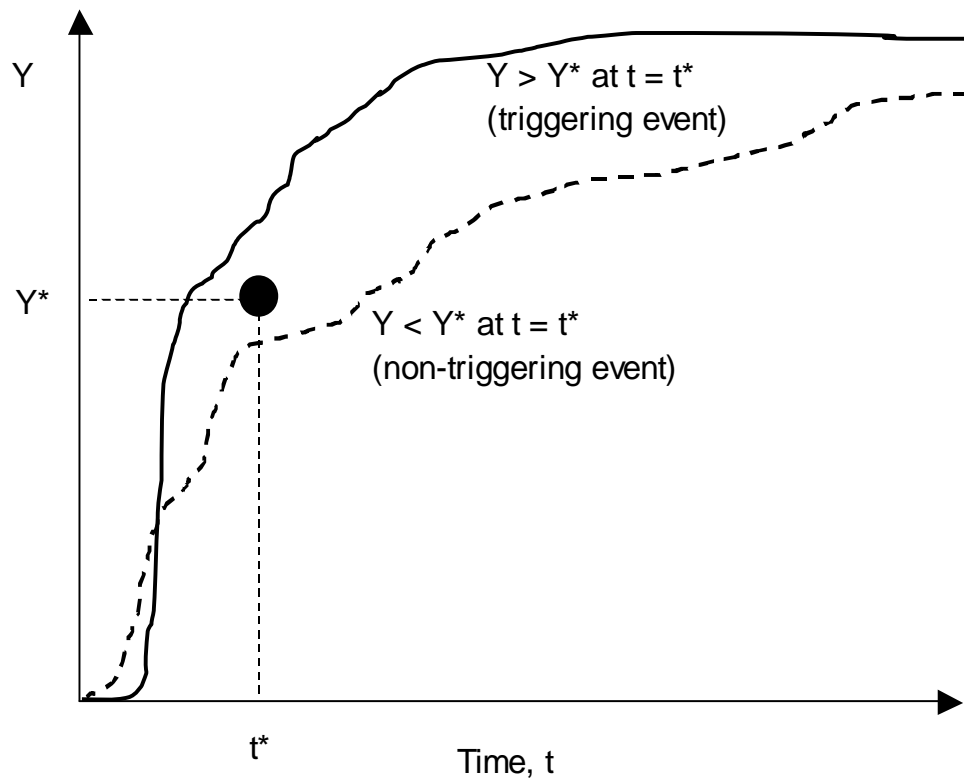
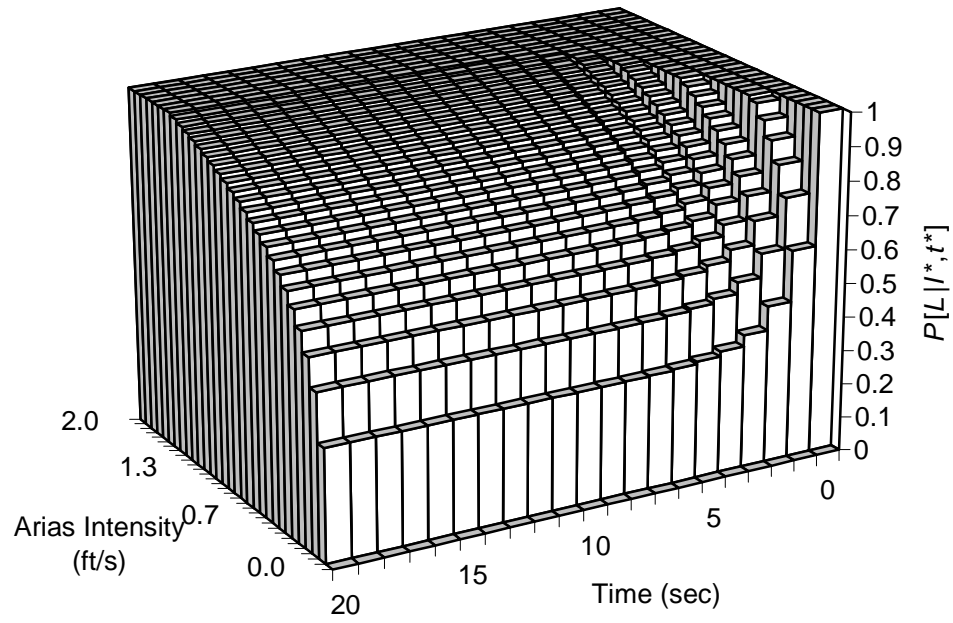
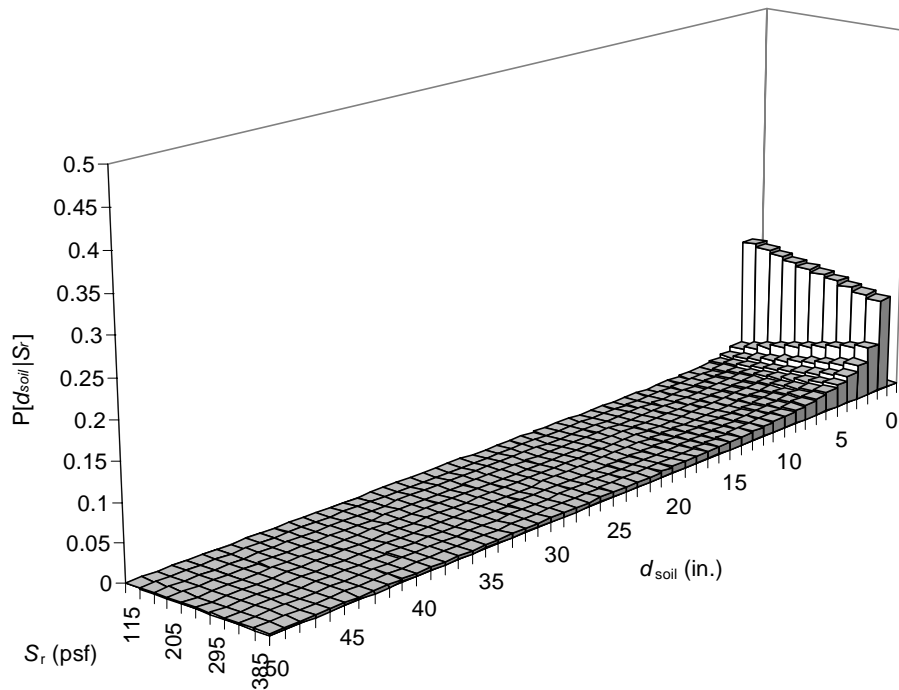


FIGURE 2 Variation of ground motion intensity with time relative to a particular trigger criterion.

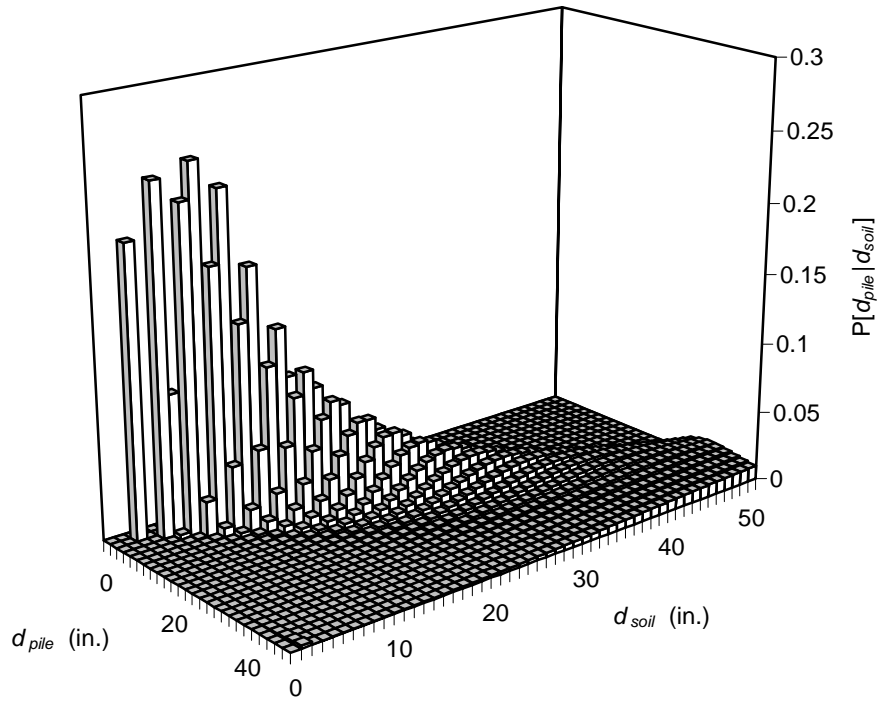


(a)

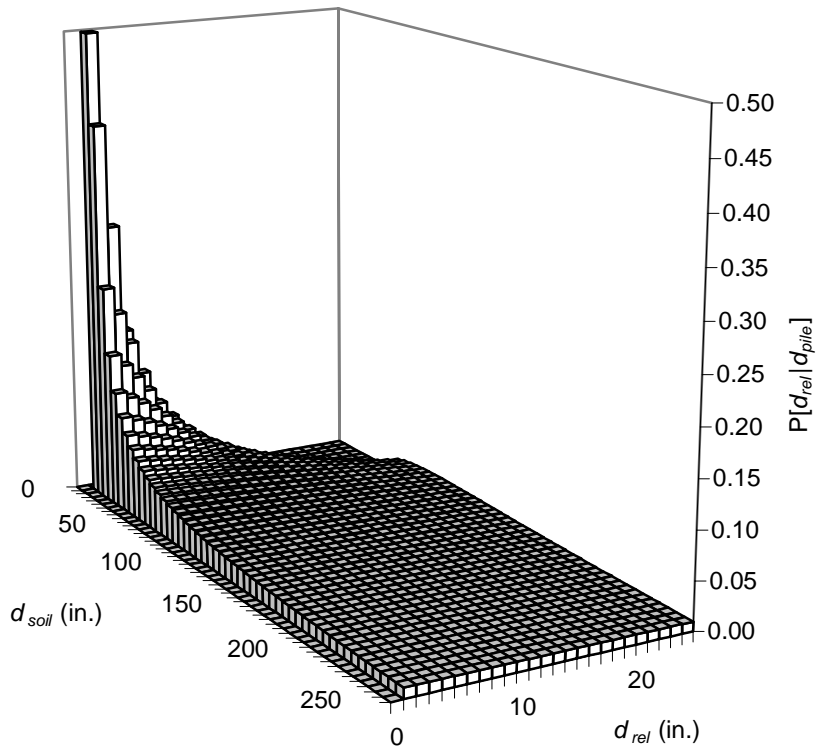


(b)

FIGURE 3 Probability density functions: (a) liquefaction given Arias intensity, and (b) seawall displacement given residual strength.

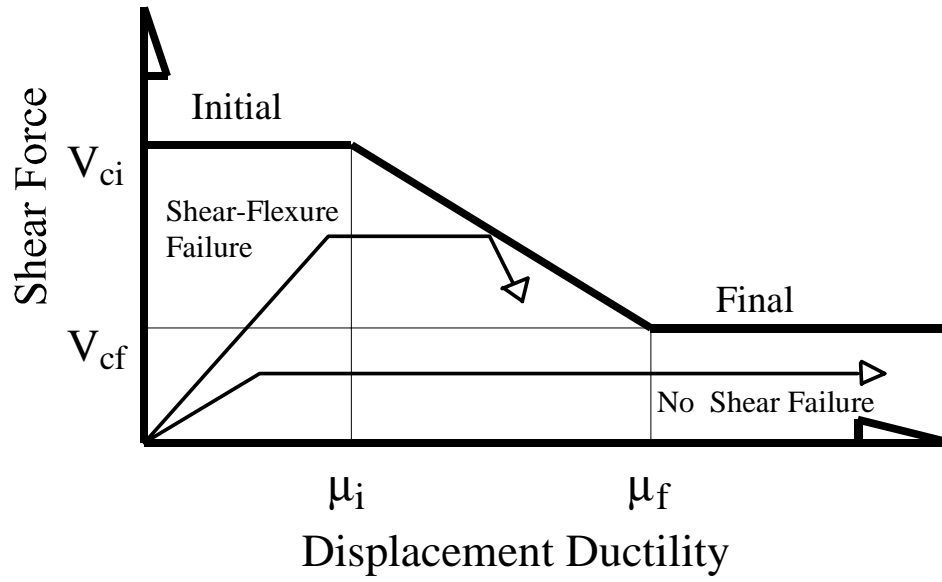


(a)

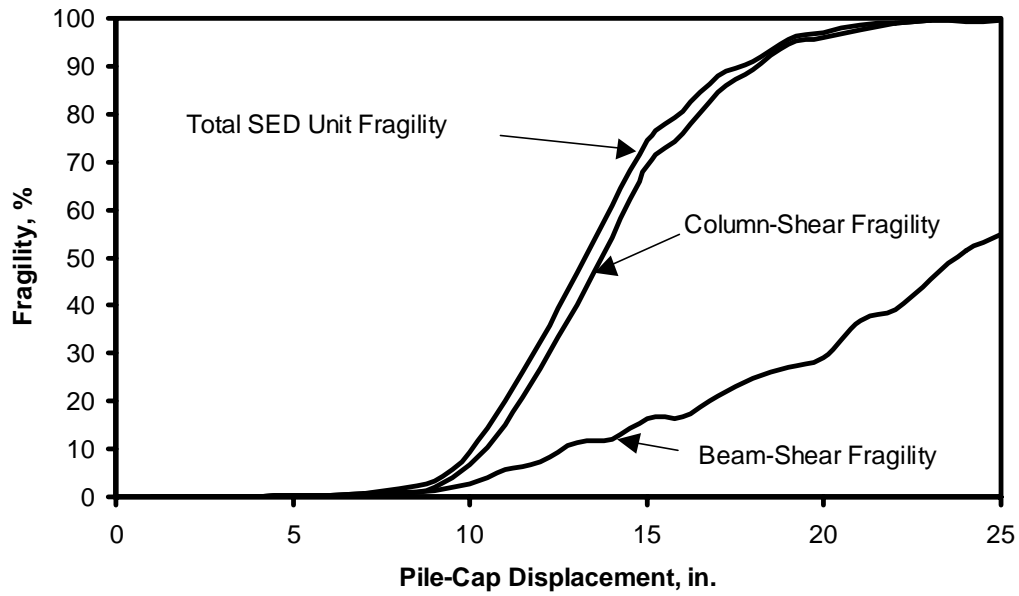


(b)

FIGURE 4 Evaluation of uncertainty in relative foundation movement: (a) pile displacement given soil displacement, and (b) relative displacement given pile displacement.



(a)



(b)

FIGURE 5 Evaluation of uncertainty in structural behavior: (a) variation of column shear resistance with displacement ductility, and (b) structural fragility curves for typical SED unit.

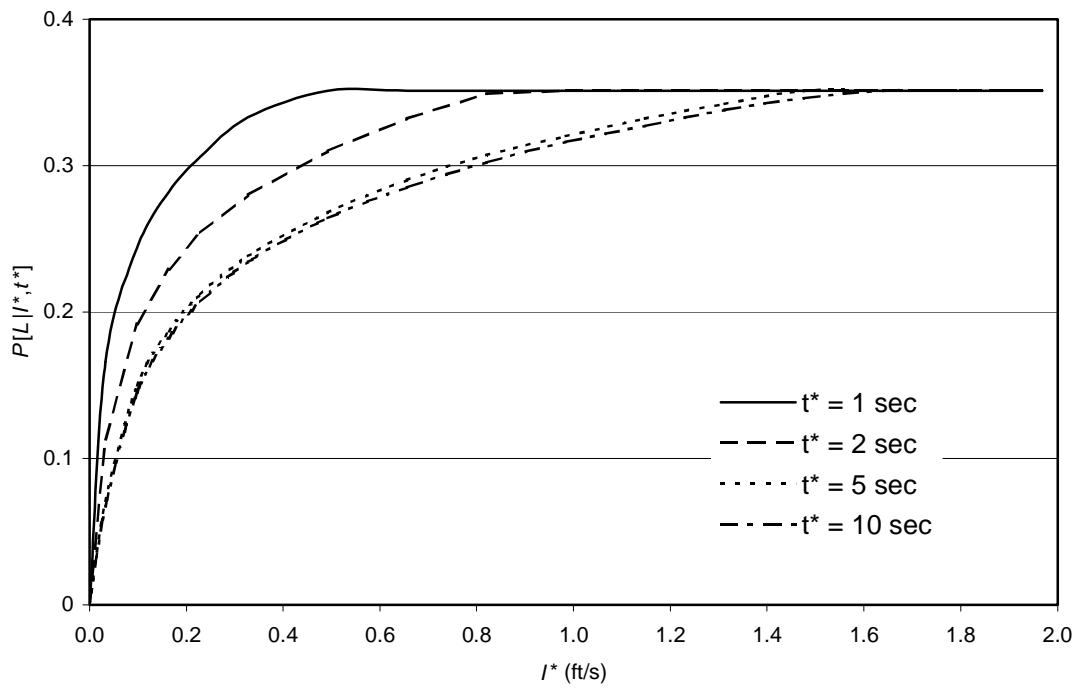


FIGURE 6 Probability of collapse considering sources of uncertainty.